

SYNTHESIS AND THERMAL PROPERTIES OF DOUBLE COMPLEX SALT: CHLOROPENTAAMMINECHROMIUM(III) BIS(OXALATO)PALLADATE

V. I. Lagunova^{1,2*}, E. Yu. Filatov¹, P. E. Plyusnin¹,
V. Yu. Komarov¹, S. A. Martynova¹,
and S. V. Korenev¹

Double complex salt $[\text{Cr}(\text{NH}_3)_5\text{Cl}][\text{Pd}(\text{C}_2\text{O}_4)_2]$ is synthesized for the first time. From the powder X-ray diffraction data it is found that the structure of the compound is triclinic with unit cell parameters: $a = 3.225(3)$ Å, $b = 10.290(6)$ Å, $c = 11.390(6)$ Å, $\alpha = 116.5(2)^\circ$, $\beta = 97.9(2)^\circ$, $\gamma = 91.2(5)^\circ$, $V = 334.5$ Å³ (room temperature). The thermal properties are studied in detail in different gaseous atmospheres using powder X-ray diffraction, IR and Raman spectroscopy to identify intermediate and final thermolysis products. The sequence of stages of the thermal destruction of the double complex salt in inert and reducing atmospheres and the formation of the final thermolysis product (a double-phase mixture of palladium and chromium(III) oxide) are established.

DOI: 10.1134/S0022476621040065

Keywords: palladium, chromium, double complex salts, thermal analysis.

INTRODUCTION

Double complex salts (DCSs) have been widely used to synthesize bimetallic nanoparticles by thermal destruction. By varying thermolysis conditions, it is possible to obtain diverse metal and metal oxide nanoparticles whose composition is strictly set by the DCS composition [1-4]. As a result of DCS decomposition, nanoparticles of metals, metallic solid solutions, or heterogeneous mixtures with various physicochemical properties are obtained, which makes it possible to apply them in different fields of science, electronics, industry, and medicine [5-8]. Thus, for instance, in the thermal decomposition of $[\text{Co}(\text{NH}_3)_6][\text{Fe}(\text{C}_2\text{O}_4)_3] \cdot 3\text{H}_2\text{O}$ in the hydrogen atmosphere the final product at 500 °C is a solid solution of the composition $\text{Co}_{0.5}\text{Fe}_{0.5}$. Thermolysis of the same compound in the argon atmosphere at 410 °C leads to the formation of a mixture of $\text{Co}_{x}\text{Fe}_{1-x}$, Fe_3O_4 , and CoFe_2O_4 [9]. Thermal destruction of $[\text{Pt}(\text{NH}_3)_5\text{Cl}][\text{ReCl}_6]\text{Cl} \cdot \text{H}_2\text{O}$ complex salt in the inert atmosphere (helium) at 840 °C is completed by the formation of two solid solutions of compositions $\text{Pt}_{0.90}\text{Re}_{0.10}$ (fcc) and $\text{Pt}_{0.25}\text{Re}_{0.75}$ (hcp) [10].

There are several works devoted to the investigation of thermal properties of complex salts containing Pt/Pd and Cr as central atoms. After the thermolysis of $[\text{Cr}(\text{NH}_3)_5\text{Cl}][\text{PtCl}_4]$ DCS in the helium atmosphere on heating to 450 °C, a mixture of platinum and chromium(III) oxide is obtained, and thermolysis in the hydrogen atmosphere at 800 °C results in the formation of a mixture of a $\text{Cr}_x\text{Pt}_{1-x}$ solid solution and fine metallic chromium that oxidizes in air with the formation of

¹Nikolaev Institute of Inorganic Chemistry, Siberian Branch, Russian Academy of Sciences, Novosibirsk, Russia;
*varvara@niic.nsc.ru. ²Novosibirsk State University, Novosibirsk, Russia. Original article submitted September 29, 2020; revised October 15, 2020; accepted November 2, 2020.

chromium(III) oxide due to pyrophoricity [11]. Thermolysis of $[\text{Cr}(\text{NH}_3)_5\text{Cl}][\text{PdBr}_4]$ leads to the formation of a mixture of the $\text{Cr}_{x}\text{Pt}_{1-x}$ solid solution and fine chromium, however, in the helium atmosphere, the decomposition temperature is 665 °C (which is caused by a higher thermal stability of intermediate bromide compounds with platinum), and in the hydrogen atmosphere, it is 450 °C [12]. In [3], it is shown that after thermolysis of $[\text{Pt}(\text{NH}_3)_5\text{Cl}][\text{Cr}(\text{C}_2\text{O}_4)_3]$ in the hydrogen atmosphere (425 °C), PtCr intermetallide is formed. During thermolysis of $[M(\text{NH}_3)_4]\text{A}$ ($M = \text{Pt}, \text{Pd}; \text{A} = \text{CrO}_4, \text{Cr}_2\text{O}_7$) in the oxygen and helium atmosphere, a mixture of Pt/Pd and Cr_2O_3 is formed, and during thermolysis in the hydrogen atmosphere, chromium is partially reduced with the formation of a $M_x\text{Cr}_{1-x}$ ($M = \text{Pt}, \text{Pd}$) solid solution with a chromium content up to 22 at.%. Products of the thermal decomposition of $[\text{Pt}(\text{NH}_3)_4]\text{Cr}_2\text{O}_7$ and $[\text{Pd}(\text{NH}_3)_4]\text{Cr}_2\text{O}_7$ in the oxygen atmosphere have shown a high catalytic activity in the processes of complete and partial oxidation of carbon monoxide in comparison with monometallic platinum and palladium catalysts [13].

Complex salt containing palladium and chromium as central atoms was synthesized. The oxalate anion enabling the prediction of the possible formation of a solid solution during thermal decomposition is chosen as one of the ligands.

EXPERIMENTAL

Starting reagents were $[\text{Cr}(\text{NH}_3)_5\text{Cl}]\text{Cl}_2$, synthesized by the procedure from [14], and $(\text{NH}_4)_2[\text{Pd}(\text{C}_2\text{O}_4)_2]$, synthesized by the procedure from [15]. To synthesize $[\text{Cr}(\text{NH}_3)_5\text{Cl}][\text{Pd}(\text{C}_2\text{O}_4)_2]$, 0.2114 g of $(\text{NH}_4)_2[\text{Pd}(\text{C}_2\text{O}_4)_2]$ (**1**) and 0.1624 g (1:1 molar ratio) of $[\text{Cr}(\text{NH}_3)_5\text{Cl}]\text{Cl}_2$ (**2**) were dissolved separately in the minimum volume of water (29 mL and 18 mL respectively). When the solutions were mixed, pink fine powder immediately precipitated. To increase the yield the solution with the precipitate was placed into an ice crystallizer for 1 h. Then the precipitate was filtered off, washed with water and acetone. The yield was 86%.

The X-ray diffraction (XRD) analysis of samples of the synthesized compounds was performed on a DRON-RM4 diffractometer (CuK_α radiation, graphite monochromator, room temperature). The samples were prepared by grinding in an agate mortar with the addition of ethanol. The suspension obtained was deposited on the polished side of the standard quartz cuvette. After drying the sample represented a thin even layer with a thickness of ~100 μm . Samples of thermolysis products were prepared similarly, however, because of their possible hygroscopicity, heptane was used during grinding. A polycrystalline silicon sample ($a = 5.4309 \text{ \AA}$) prepared similarly was used as the external standard. XRD patterns were measured in a step-by-step mode ($\Delta 2\theta = 0.1^\circ$, point acquisition time 6 s) in the 2θ angle range from 5° to 60° for complex salts and from 5° to 95° for thermolysis products.

The phase composition of metallic thermolysis products was established by analyzing the positions of separate reflections (a description of the peak profile by the pseudo-Voigt function) in the 2θ angle range from 60° to 95°, where the measurement error of the interplanar distance is minimum. Metallic and oxide phases were indexed by analogy with XRD patterns of pure compounds, according to the PDF database [16].

Unit cell parameters of $[\text{Cr}(\text{NH}_3)_5\text{Cl}][\text{Pd}(\text{C}_2\text{O}_4)_2]$ were indexed by the positions of maxima of the main peaks up to 2θ 35° and refined by the Pauli method using the TOPAS-Academic V6 program [18]. The most probable variant of indexation corresponded to the triclinic system: $a = 3.225(3) \text{ \AA}$, $b = 10.290(6) \text{ \AA}$, $c = 11.390(6) \text{ \AA}$, $\alpha = 116.5(2)^\circ$, $\beta = 97.9(2)^\circ$, $\gamma = 91.2(5)^\circ$, $V = 334.5 \text{ \AA}^3$. The correctness of the variant found was confirmed by the indexation of diffraction peaks measured for a polycrystalline microcrystal (linear dimensions < 3 μm) to $d = 2.5 \text{ \AA}$ on a three-circle Bruker D8Venture single crystal diffractometer (IμS 3.0 CuK_α , PHOTON III detector) using the APEX3 program package [19].

Lattice parameters of thermolysis products were refined by the full-profile method over the entire set of reflections using PowderCell 2.4 [17] and TOPAS-Academic V6 [18] applied programs. CSR sizes of metallic phases were determined by the Fourier profile analysis of single diffraction peaks and by the Scherrer formula (WINFIT 1.2.1 program) [20].

IR spectra of DCS and intermediate thermolysis products were measured on a Bruker Vertex 80 Fourier spectrometer in the wavenumber range 400-4000 cm⁻¹ in KBr pellets and in the range 80-600 cm⁻¹ in spectroscopic polyethylene pellets. IR spectral bands were assigned by comparing with the reported data [21-23].

The thermogravimetric analysis (TGA) was carried out on a TG 209 F1 Iris (NETZSCH, Germany) instrument. The simultaneous thermal analysis TG-DSC/EGA-MS (thermogravimetry, differential scanning calorimetry, and mass spectrometry with the analysis of releasing gases) was carried out on an apparatus consisting of an STA 449 F1 Jupiter thermal analyzer and a QMS 403D Aeolos (NETZSCH, Germany) quadrupole mass spectrometer. Measurements were performed in Al₂O₃ crucibles in a helium flow and in a hydrogen-helium mixture (10 vol.% H₂ in He) in the temperature range 30-900 °C at a heating rate of 10 K/min and a gas flow rate of 60 mL/min. Experimental data were processed using the standard Proteus program package.

RESULTS AND DISCUSSION

Thermal decomposition of the main mass of [Cr(NH₃)₅Cl][Pd(C₂O₄)₂] in the hydrogen atmosphere proceeds in three stages that are poorly separated from each other (Fig. 1). The first occurs in the temperature range 170-230 °C and is accompanied by release of water and ammonia, which indicates a destruction of chromium and palladium coordination spheres. In the XRD pattern of a sample prepared by heating to 200 °C with subsequent rapid cooling to room temperature, low-intensity reflections of initial DCS are observed. According to the vibrational spectroscopy results, IR spectra of the intermediate thermolysis product at 200 °C practically do not change in the far and middle regions as compared to the initial complex. However, the intensity of some lines in the Raman spectrum changes significantly in the range 1000-200 cm⁻¹, which seems to be due to symmetry violation of the coordination sphere of central atoms caused by thermolysis. These changes indicate the onset of DCS decomposition. The main vibrational frequencies and their assignment for the [Cr(NH₃)₅Cl][Pd(C₂O₄)₂] complex as well as its thermolysis products are presented in Table 1 and Fig. 2.

The second stage of decomposition takes place in the temperature range 230-340 °C. Here the palladium coordination sphere is destructed and palladium is reduced to the zero-valent state. The main gaseous products detected in the mass spectrum are CO₂ and H₂O; moreover, the release of some amount of ammonia is observed. The XRD pattern of the intermediate decomposition product obtained at 250 °C (Fig. 3) exhibits residual reflections from the initial complex

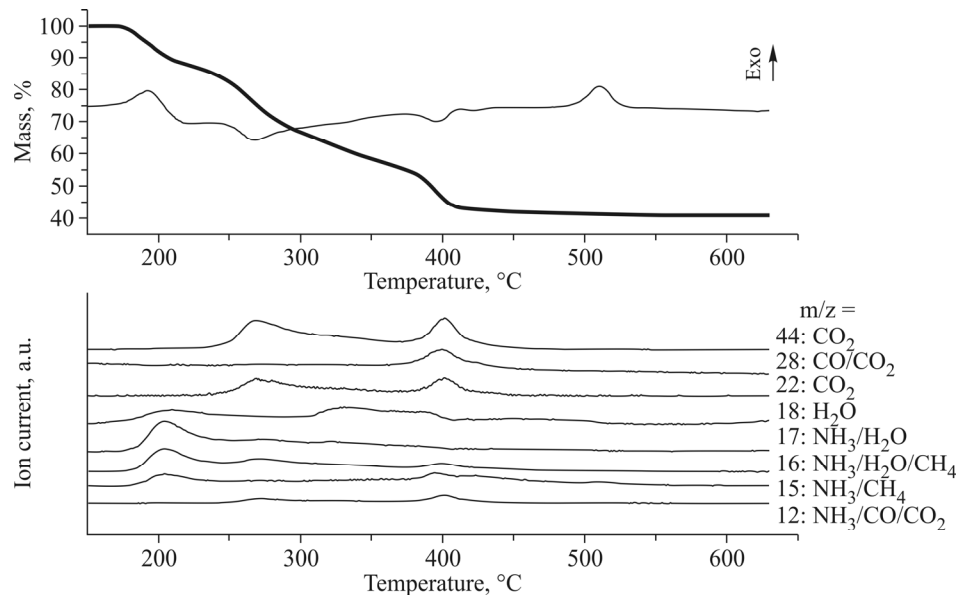


Fig. 1. TGA curves of [Cr(NH₃)₅Cl][Pd(C₂O₄)₂] in the reducing atmosphere, 10 K/min.

TABLE 1. Main Vibrational Frequencies and Their Assignment for the $[\text{Cr}(\text{NH}_3)_5\text{Cl}][\text{Pd}(\text{C}_2\text{O}_4)_2]$ Complex, and Also the Products of Its Thermolysis in the Hydrogen Atmosphere at Different Temperatures

Band assignment	$\text{K}_2[\text{Pd}(\text{C}_2\text{O}_4)_2] \cdot 2\text{H}_2\text{O}$ [21, 22]	$[\text{Cr}(\text{NH}_3)_5\text{Cl}][\text{IrCl}_6]$ [22, 23]	$[\text{Cr}(\text{NH}_3)_5\text{Cl}][\text{Pd}(\text{C}_2\text{O}_4)_2]$ (I)	Heating of (I) in the H_2 atm.			
				to 200 °C	to 250 °C	to 350 °C	to 450 °C
$\nu(\text{NH}_3)$	—	3289	3308 s.	3308	3308	—	—
$\nu(\text{NH}_3)$	—	3226	3248 sh.	3248 sh.	3238	3238	—
$\nu(\text{NH}_3)$	—	3154	3176	3176	3179	—	—
$\nu(\text{C=O})$	1698	—	1707	1707	1711	1709	—
$\delta_{\text{as}}(\text{NH}_3)+/\text{or}$	1675	1676 sh.	1682	1682	1678 b.	—	—
$\nu(\text{C=O})$	—	—	—	—	—	—	—
$\nu(\text{C=O})$	1657	—	1655	1653	—	1655 b.	1639 b.
$\delta_{\text{as}}(\text{NH}_3)$	—	1606	1613	1612	1615	—	—
$\nu_s(\text{C-O})+/\text{or}$	1394	—	1405	1402	1435 sh.	1423	1454
$+v_s(\text{CC})$	—	—	1389	1389	1395	—	—
		1377 sh.	1375 sh.	—	—	—	—
$\nu_s(\text{C-O})$	—	—	1348	1348	—	1342	—
$\delta_s(\text{NH}_3)$	—	1304	1312	1314	—	1315	—
$\delta_s(\text{NH}_3)$	—	1292	1285	1285	1276 sh.	1296 b.	—
$\delta_s(\text{NH}_3)$	—	1261	1249	1250	1261 b.	—	—
$\nu(\text{C-O})+/\text{or}$	1245	—	1238	1238	—	—	—
$\nu(\text{C-O})$	—	—	—	—	1096	1078	—
$\nu(\text{C-O})$	—	—	—	—	1028	1046	1043
$\nu_s(\text{C-O})$	—	—	914	916	903	912	—
$\nu_s(\text{CO})+/\text{or}$	893	—	891	893	—	—	—
$+v(\text{OCO})$	—	—	—	—	—	—	—
$\delta(\text{OCO})+/\text{or}$	818	—	818	817	812	812	—
$+v(\text{PdO})$	—	—	—	—	—	—	—
$\delta(\text{NH}_3)$	—	766	782	783	—	768	—
		745	745	—	—	—	—
$\nu(\text{PdO})+/\text{or}$	556	—	555	IR/561 RR	552	550	559
$+v_s(\text{CC})$	—	—	—	—	—	—	—
$\nu(\text{CrO})$	—	—	—	—	—	—	548b.
		—	—	—	—	—	IR/562 RR
$\text{Ring def.}+/\text{or}$	469	—	465	467	488	474	—
$+v(\text{OCO})$	—	—	IR/495 RR	—	—	—	—
$\nu(\text{CrN})$	—	455	440	440	—	—	—
$\nu(\text{CrN})+/\text{or}$	417	425	415	415	415	411	—
$(\nu(\text{PdO})+/\text{or}$	—	—	—	—	—	—	—
$+v(\text{CC})$	368	—	354	355	377	—	—
$+v(\text{OCO})$	350	—	—	—	—	—	—
$\nu(\text{CrCl})$	—	306	300	301	—	—	—
$\delta(\text{NCrN})$	—	—	269	—	—	—	—
$\delta(\text{NCrN})$	—	—	240	241	247	—	—

s. – strong, b. – broad, sh. – shoulder.

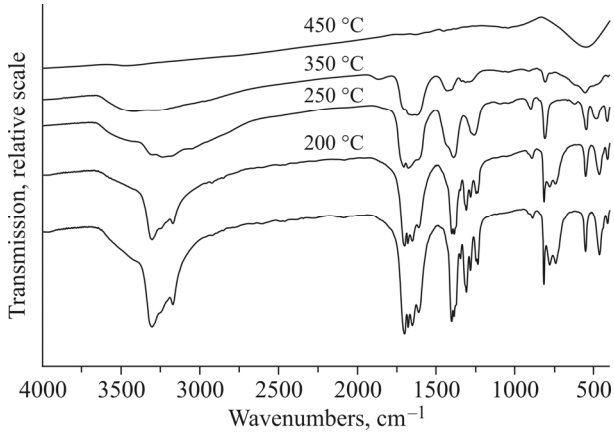


Fig. 2. IR spectrum of the $[\text{Cr}(\text{NH}_3)_5\text{Cl}][\text{Pd}(\text{C}_2\text{O}_4)_2]$ complex and products of its thermal decomposition in the reducing atmosphere (hydrogen atmosphere at different temperatures).

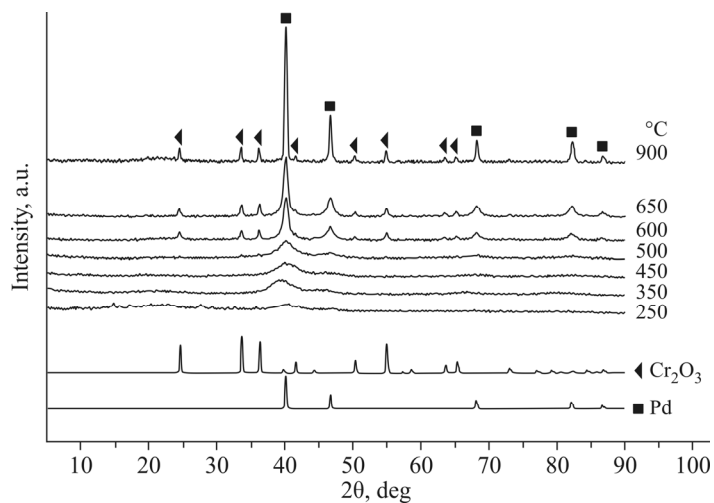


Fig. 3. XRD patterns of $[\text{Cr}(\text{NH}_3)_5\text{Cl}][\text{Pd}(\text{C}_2\text{O}_4)_2]$ thermolysis products in the hydrogen atmosphere at different temperatures.

compound, a background rise in the range of angles corresponding to reflections of fine palladium and low-intensity reflections of NH_4Cl (bands characteristic of NH_4Cl are not detected in the IR spectra). The third stage of thermal destruction proceeds in the temperature range 340–450 °C. Here the main gaseous product released is CO. Furthermore, H_2O , CO_2 , and insignificant amounts of ammonia are released.

In the XRD pattern of the product obtained at 350 °C, a halo of the amorphous phase appears, and a shift of reflections of the fcc palladium phase to smaller angles is observed because hydrogen partially enters the structure of palladium and PdH_x is formed ($a = 4.014(3)$ Å). According to the data published, the $\text{PdH}_{0.64}$ unit cell parameter is 4.03 Å [24], and for $\text{PdH}_{0.706}$ it is 4.035 Å [25]. The thermal decomposition process ends at 450 °C. Further heating to 900 °C is accompanied by an insignificant decrease in mass, which we explain by the removal of residual amounts of carbon formed during thermal destruction of the oxalate ion. At 450 °C the XRD pattern exhibits a broad reflection of the amorphous phase, and an inverse shift of PdH_x reflections to large angles is also observed due to the decomposition of palladium hydride. Vibrational spectroscopy data agree well with and confirm powder XRD and thermal analysis data. In the spectra of

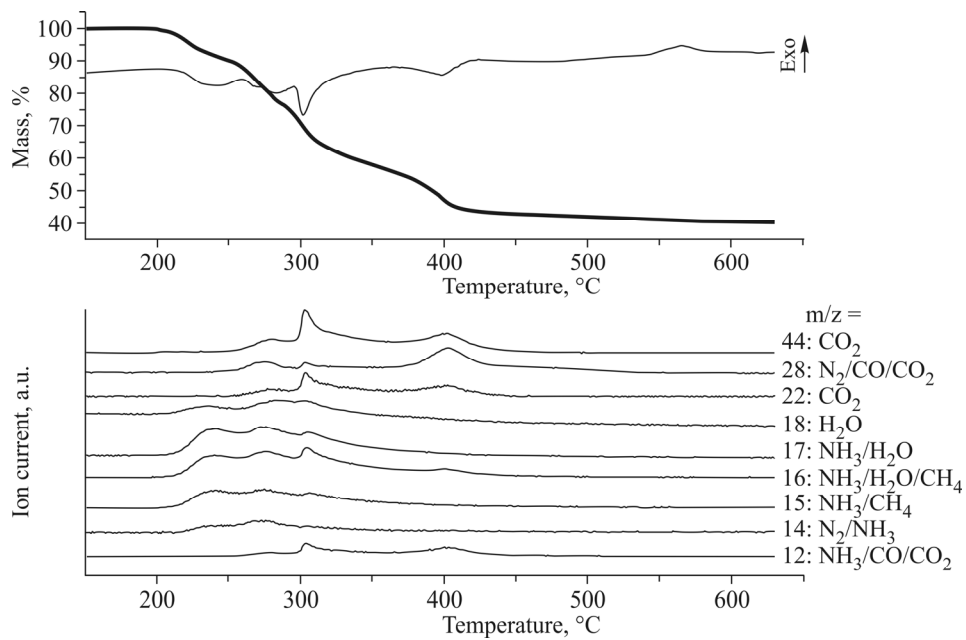


Fig. 4. TGA curves of $[\text{Cr}(\text{NH}_3)_5\text{Cl}][\text{Pd}(\text{C}_2\text{O}_4)_2]$ in the inert atmosphere, 10 K/min.

intermediate products at 250 °C, 350 °C, and 450 °C, a gradual decrease in the intensity is observed, and then stretching and bending vibrational bands of the ammine group disappear. At a temperature above 250 °C, noticeable changes in vibrations of the oxalate ligand start to occur. Changes in the intensity and the disappearance of vibrations corresponding to the ammine group take place before the change in the intensity of lines corresponding to the oxalate ligand. The spectrum of the thermolysis product at 450 °C demonstrates a strong and intense band corresponding to $\nu(\text{Cr}-\text{O})$ vibrations. According to the published data [21-23], the position of the mentioned line corresponds to Cr(III). In the temperature range 470-550 °C (onset 493 °C), an exo effect is observed, which is related to the crystallization of amorphous chromium(III) oxide. At 500 °C the XRD pattern contains only the reflections of metallic palladium ($\text{CSR} = 2-3 \text{ nm}$), and already at 600 °C the reflections of chromium(III) oxide appear. Further heating enlarges metallic palladium particles. The size of fcc phase particles was estimated by CSR sizes and is 5-8 nm at 650 °C. The final product of decomposition at 900 °C is a mixture of metallic palladium (19-27 nm) and chromium(III) oxide (21-30 nm).

Decomposition of DSC in the inert atmosphere (Fig. 4) is in general similar to that in the reducing atmosphere. The distinction is an elevation of the decomposition onset temperature and the participation in redox processes of ammonia molecules. Decomposition begins at 195 °C and is accompanied by the release of water, ammonia, and insignificant amounts of N₂, which as in the reducing atmosphere, indicates the onset of the destruction of chromium and palladium coordination spheres. In the temperature range 250-290 °C the second stage of decomposition proceeds, which is accompanied by the release of water, ammonia, CO and CO₂ (in comparable amounts), and insignificant amounts of N₂. At this stage, the destruction of chromium and palladium coordination spheres continues. The third stage proceeds in the range 290-360 °C. Here the main gaseous products are water and CO₂, with CO, NH₃, and insignificant amounts of nitrogen being detected, too. In the temperature range 360-450 °C there is the fourth stage of the thermolysis that results in the complete decomposition of intermediate products formed. Here the main gaseous products are CO and CO₂. Further heating to 900 °C is accompanied by an insignificant weight loss caused by the removal of residual amounts of carbon formed during the thermal destruction of the oxalate ion. The final decomposition product, as in the case of the reducing atmosphere, is a mixture of metallic palladium and chromium(III) oxide. In the inert atmosphere, amorphous chromium(III) oxide also crystallizes at higher temperatures in the range 500-600 °C and is accompanied by an exo effect (Onset 544 °C).

CONCLUSIONS

Thus, in the reducing and inert atmospheres, the thermal decomposition of $[\text{Cr}(\text{NH}_3)_5\text{Cl}][\text{Pd}(\text{C}_2\text{O}_4)_2]$ occurs similarly. At the same time, chromium and palladium coordination spheres are destructed, which is confirmed by a number of physicochemical methods of analysis. The reduction of chromium to the metallic state and the formation of $\text{Pd}_x\text{Cr}_{1-x}$ solid solutions were not detected, however, a method to synthesize nanoscale composite materials with a catalytic activity has been developed. It is also shown that during thermolysis in the hydrogen atmosphere, the formation of palladium nanoparticles is accompanied by the formation of palladium hydride that decomposes with increasing temperature.

CONFLICT OF INTERESTS

The authors declare that they have no conflict of interests.

REFERENCES

1. A. V. Zadesenets, E. Y. Filatov, P. E. Plyusnin, T. I. Asanova, I. V. Korolkov, I. A. Baidina, E. V. Shlyakhova, I. P. Asanov, and S. V. Korenev. *New J. Chem.*, **2018**, *42*, 11, 8843.
2. A. V. Zadesenets, A. B. Venediktov, S. V. Korenev, I. A. Baidina, and S. A. Gromilov. *J. Struct. Chem.*, **2005**, *46*(6), 1091.
3. K. V. Yusenko, D. B. Vasil'chenko, A. V. Zadesenets, I. A. Baidina, Y. V. Shubin, and S. V. Korenev. *Russ. J. Inorg. Chem.*, **2007**, *52*(10), 1487.
4. S. V. Korenev, A. B. Venediktov, Yu. V. Shubin, S. A. Gromilov, and K. V. Yusenko. *J. Struct. Chem.*, **2003**, *44*(1), 46.
5. D. I. Potemkin, E. S. Saparbaev, A. V. Zadesenets, E. Y. Filatov, P. V. Snytnikov, and V. A. Sobyanin. *Catal. Ind.*, **2018**, *10*(1), 62.
6. C. Hu, Z. Chen, F. Han, Z. Lin, and X. Yang. *Chem. Commun.*, **2019**, *55*(90), 13566.
7. L. Yang, L. Chen, Y. C. Chen, L. Kang, J. Yu, Y. Wang, C. Lu, T. Mashimo, A. Yoshiasa, and C. H. Lin. *Colloids Surf., B*, **2019**, *180*(64), 466.
8. K. Yatsugi, T. Ishizaki, K. Akedo, and M. Yamauchi. *J. Nanopart. Res.*, **2019**, *21*, 3.
9. Y. P. Semushina, P. E. Plyusnin, Y. V. Shubin, S. I. Pechenyuk, and Y. V. Ivanov. *J. Struct. Chem.*, **2015**, *64*(8), 1963.
10. A. V. Zadesenets, I. V. Korol'kov, and S. A. Gromilov. *J. Struct. Chem.*, **2013**, *54*(1), 201.
11. P. E. Plusnin, Y. V. Shubin, K. V. Yusenko, I. A. Baidina, T. M. Korda, and S. V. Korenev. *Russ. J. Inorg. Chem.*, **2004**, *49*(8), 1148.
12. Y. V. Shubin, A. V. Zadesenets, A. B. Venediktov, and S. V. Korenev. *Russ. J. Inorg. Chem.*, **2006**, *51*(2), 202.
13. E. Y. Filatov, V. Lagunova, D. Potemkin, N. Kuratieva, A. Zadesenets, P. Plyusnin, A. Gubanov, and S. Korenev. *Chem. – Eur. J.*, **2020**, *26*(19), 4341.
14. Handbook of Preparative Inorganic Chemistry / Ed. G. Brauer. Academic Press, **1963**.
15. G. Landesen. *Z. Anorg. Allg. Chem.*, **1926**, *154*(1), 429.
16. Powder Diffraction File, PDF-2. International Centre for Diffraction Data: Newtown, Pennsylvania, USA, **2014**.
17. A. A. Coelho. TOPAS-Academic, Version 6.0 (Computer Software). Coelho Software: Brisbane, **2019**.
18. APEX3, Version 2018.7-2. Bruker AXS: Madison, Wisconsin, USA, **2005–2018**.
19. W. Kraus and G. Nolze. PowderCell 2.4. Program for the Representation and Manipulation of Crystal Structures and Calculation of the Resulting X-Ray Powder Patterns. Federal Institute for Materials Research and Testing: Berlin, Germany, **2000**.
20. S. Krumm. *Mater. Sci. Forum*, **1996**, 228–231, 183.

21. K. Nakamoto. Infrared and Raman Spectra of Inorganic and Coordination Compounds: Part B: Applications in Coordination, Organometallic, and Bioinorganic Chemistry, 6th edition. John Wiley & Sons: New York, **2009**.
22. J. Fujita, A. E. Martell, and K. Nakamoto. *J. Chem. Phys.*, **1962**, *36*, 324.
23. S. A. Martynova, P. E. Plyusnin, T. I. Asanova, I. P. Asanov, D. P. Pishchur, S. V. Korenev, S. V. Kosheev, S. Floquet, E. Cadot, and K. V. Yusenko. *New J. Chem.*, **2018**, *42*, 1762.
24. Y. P. Khodyrev, R. V. Baranova, R. M. Imamov, and S. A. Semiletov. *Izv. Akad. Nauk SSSR, Neorg. Mater.*, **1978**, *14*, 1645.
25. J. E. Worsham, M. G. Wilkinson, and C. G. Shull. *Phys. Chem. Solids*, **1957**, *3*, 303.